

# OPTIMIZED DESIGN AND AERODYNAMIC PERFORMANCE ANALYSIS OF WIND TURBINE BLADES WITH SPARROWHAWK BIONIC AIRFOIL

Yuanjun DAI<sup>1,4\*</sup>, Dong WANG<sup>1</sup>, Xiongfei LIU<sup>2</sup>, Weimin WU<sup>3,4</sup>

*This article utilizes the biomimetic approach to establish a biologically inspired airfoil profile for a sparrowhawk and compare its lift-to-drag ratio to that of the NACA6409 airfoil profile. The airfoil sections for wind turbine blades are obtained through a non-uniform distribution method. Based on this approach, a mathematical model is developed for optimizing the design of wind turbine blades. MATLAB software is used to calculate the external parameters and three-dimensional coordinates of each airfoil section, which are then imported into SolidWorks software for precise modeling. Additionally, computational analysis is conducted to evaluate the aerodynamic performance of the blades.*

**Keywords:** Airfoil; Wind turbines; Blade design

## 1. Introduction

Energy plays a critical role in supporting human social development and economic growth. Wind energy, regarded as a sustainable and environmentally friendly source, has gained increasingly significant attention [1,2]. Wind turbine blades are crucial components for transforming wind energy into mechanical energy, and their design and performance significantly impact the efficiency of the

<sup>1</sup> School of Mechanical Engineering, Shanghai DianJi University, China, e-mail: 24354267@qq.com. (corresponding author)

<sup>2</sup> School of Information Engineering, Yinchuan University of Science and Technology, China, e-mail: 252860420@qq.com.

<sup>3</sup> School of Mechanical and Power Engineering, Chongqing University of Science and Technology, China, e-mail: 2019008@cqust.edu.cn.

<sup>4</sup> School of Aeronautical Mechanical and Electrical Engineering, Chongqing Aerospace Polytechnic, China, e-mail: 24354267@qq.com.

wind power generation system. Optimizing blade design allows for efficient capture and utilization of wind energy while improving the energy conversion rate and the performance of wind power generation [3,4].

There are two main approaches to enhance the aerodynamic performance of wind turbine blades. The first is the development of new airfoils specifically designed for wind turbines or the improvement and optimization of existing airfoils. The second approach involves enhancing blade design methods. Y. Zhiqiang et al. [5] proposed a design optimization method for vertical-axis wind turbine airfoils that considers multiple angles of attack. The method focuses on utilizing the concentrated distribution of inflowing wind energy to enhance the lift-to-drag ratio at various angles of attack positions, thereby further optimizing the aerodynamic performance of the airfoil. Yuan K S et al. [6] proposed a method to enhance the aerodynamic performance of wind turbine blades by refining the trailing edge of the airfoil. Huang S et al. [7] proposed modifying the leading edge of the NACA0018 airfoil to create a new airfoil with a shape resembling that of a dolphin's head. They made adjustments, optimizations, and conducted an analysis of the aerodynamic function of the modified airfoil, ultimately achieving improved aerodynamic performance at a deflection angle of 24°. Hua X et al. [8] employed seagull-inspired airfoils to design bionic wind turbine blades and subsequently assessed their aerodynamic performance. The results indicated an increase in torque at different wind speeds for the modified airfoil. Tian W et al. [9] designed an airfoil inspired by the long-eared owl and employed the Glauert model to create a bionic blade. Numerical simulations demonstrated a 12% increase in efficiency for the optimized blade compared to standard ones. Airfoil optimization and design for enhancing aerodynamic performance have been conducted by L. Wenzhi et al. [10], Yan H. et al. [11], Hassanzadeh, A et al. [12], and others. However, these aforementioned articles focused on airfoil optimization and design, without addressing the improvement of design methods for wind turbine blades.

Sang-Lae Lee et al. [13] examined various design parameters and utilized the second-order response surface method to establish the correlation between the objective function and factors such as chord length and torsion angle in the design calculations. They compared the performance of the optimized blade with the original design and found significant improvements. Li Q et al. [14] presented an overview of wind turbine aerodynamic theory and aerodynamic calculation models. They discussed both traditional shape optimization methods and modern optimization techniques in aerodynamic design. Rodriguez Christian V [15]

proposed an integrated optimization methodology for wind turbine blade design by combining computational fluid dynamics (CFD), blade element momentum theory (BEM), and genetic algorithms (GA). Zhu, Jie et al. [16] proposed a MATLAB-based program combined with Ansys to achieve an optimal trade-off between maximum power generation and minimum blade mass in wind turbine design. Zhang B et al. [17], Maki K [18], Tang X et al. [19], among others, have made modifications to the wind turbine blade design methods; however, they have not made advancements in terms of airfoil design. While these articles have contributed to the methodology and optimization of wind turbine design, none of them specifically focused on the design and optimization of the wind turbine airfoil.

This paper focuses on the research and design of a Sparrowhawk bionic airfoil, conducting a lift-to-drag ratio analysis in comparison with the NACA6409 airfoil. Additionally, it aims to improve Wilson's method for blade designing through non-uniform foliation adoption and optimize the blade design to enhance wind energy capture and utilization. The ultimate goal is to improve wind power generation efficiency and achieve higher energy conversion rates. These advancements have the potential to promote more efficient utilization of renewable energy, reduce dependence on conventional energy sources, and drive innovation and progress in the renewable energy industry.

## **2. Extraction and aerodynamic performance analysis of the bionic airfoil type of sparrowhawk**

Birds are known for their exceptional flight adaptations, which include airfoil shapes that have naturally evolved to optimize flight capabilities. The airfoils of the sparrowhawk consist of a lateral arrangement of airfoil shapes that generate lift and propel the body forward through fluttering and strategic aerodynamic principles, resembling the operating conditions of wind turbines. This study utilizes a portable 3D scanner to scan the sparrowhawk airfoils and acquire a point cloud image. The resulting scan data is processed using image processing software called Image-ware, as shown in Fig. 1. Subsequently, the processed point cloud data was employed in Geomagic Studio to construct a precise three-dimensional model of the sparrowhawk airfoil. The airfoil profile was then extracted, optimized for standardization, and illustrated in Fig. 2. The coordinates of the sparrowhawk airfoil were exported from Geomagic Studio to Profili software for the establishment of the biomimetic airfoil model, as illustrated in Fig. 3. In addition, MATLAB software was employed to fit the coordinates of both the upper and lower airfoil

profiles, resulting in the derivation of an equation representing the airfoil profile coordinates.



Fig. 1 Sparrowhawk airfoil scanning process

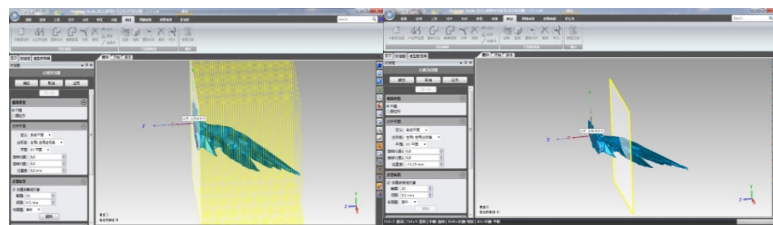


Fig. 2 Extraction process of sparrowhawk airfoil type



Fig. 3 Sparrowhawk airfoil type QY-7305

The airfoil is named QY-7305, where “QY” represents the initial capitalization of the Chinese name of the Sparrowhawk and “7305” indicates the cross section at -73.05mm with the characteristic plane as the reference.

In this paper, the aerodynamic performance of the QY-7305 airfoil is compared and analyzed with the NACA6409 airfoil, which shares similar sweep and thickness characteristics with the QY-7305 airfoil, using the Computational Fluid Dynamics (CFD) method. The division of the airfoil was conducted in ICEM-CFD using an O-shaped structured mesh. The computational domain is 10 times the chord length, and the grid is refined on the wall surface of the airfoil. This paper conducts an aerodynamic performance analysis of airfoils at different Reynolds numbers. By employing Y+ Wall Distance Estimation, parameters such as free-stream velocity and Y+ values were set to obtain the first layer grid height corresponding to the desired Reynolds number. Figures 4 and 5 depict the grid structures for the QY-7305 and NACA6409 airfoils with a Reynolds number of  $8 \times 10^5$  and a first layer grid height of  $2.8 \times 10^{-5}$ m.

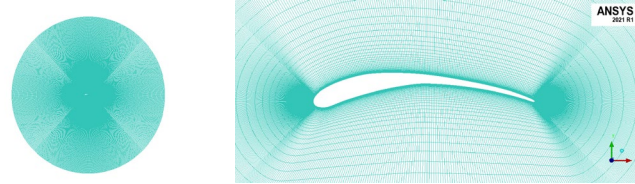


Fig. 4 QY-7305 airfoil overall grid and local grid diagram

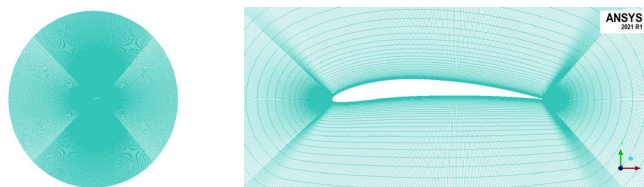


Fig. 5 NACA6409 airfoil overall grid and local grid diagram

The aerodynamic performance of the two airfoil types mentioned above was computed and analyzed using Fluent. Employing the pressure far-field approach as the boundary conditions. The airfoil is set to the adiabatic no-slip condition. The analysis focuses on varying the incoming angle of attack, specifically examining the range of 0-12 degrees in this paper. Figs. 6 and 7 display the pressure clouds of the QY-7305 and NACA2412 airfoils at 0°, 6°, and 12° angle of attack. Taking the 0° angle of attack as an example, the pressure on the upper surface of the QY-7305 airfoil is approximately -106 Pa, while the pressure on the lower surface is around 24 Pa, resulting in a pressure difference of 130 Pa. On the other hand, the NACA6409 airfoil exhibits a pressure of about -65 Pa on the upper surface and approximately 5 Pa on the lower surface. Consequently, the pressure difference amounts to approximately 70 Pa for the NACA6409 airfoil. Notably, at a 0° angle of attack, the QY-7305 airfoil displays a larger pressure difference, indicating higher lift.



Fig. 6 Pressure field of QY-7305 airfoil at angles of attack of 0°, 6° and 12°

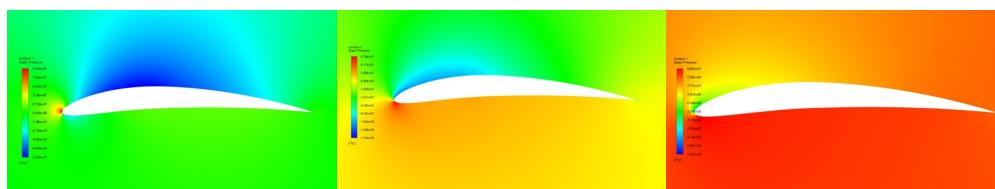


Fig. 7 Pressure field of NACA6409 airfoil at angles of attack of 0°, 6° and 12°

The lift-to-drag ratio is an indicator used to evaluate the aerodynamic performance of the airfoil. Fig. 8 depicts the characteristic curve of the lift-to-drag ratio for the QY-7305 airfoil and the NACA6409 airfoil across angles of attack ranging from 0 to 12 degrees. From the figure, it is evident that the lift-to-drag ratio of the QY-7305 airfoil at the optimal angle of attack is higher than that of the NACA6409 airfoil at the optimal angle of attack. Additionally, the QY-7305 airfoil exhibits a higher lift-to-drag ratio across a wider range of angles of attack compared to the NACA6409 airfoil.

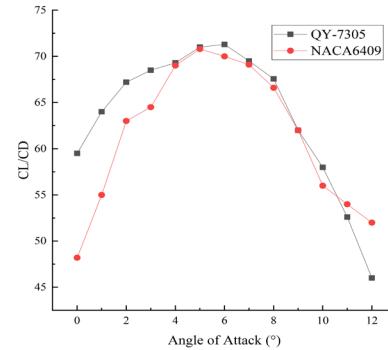


Fig. 8 Comparative analysis of lift-to-drag ratio of airfoil

The above describes the calculation and comparative analysis of the aerodynamic performance of the airfoils at a Reynolds number of  $8 \times 10^5$ . Using the same computational approach, the aerodynamic performance of the two airfoil types was calculated at Reynolds numbers of  $7.5 \times 10^5$ ,  $8.5 \times 10^5$ ,  $9 \times 10^5$ ,  $9.5 \times 10^5$ . The results of these calculations are shown in Figure 9.

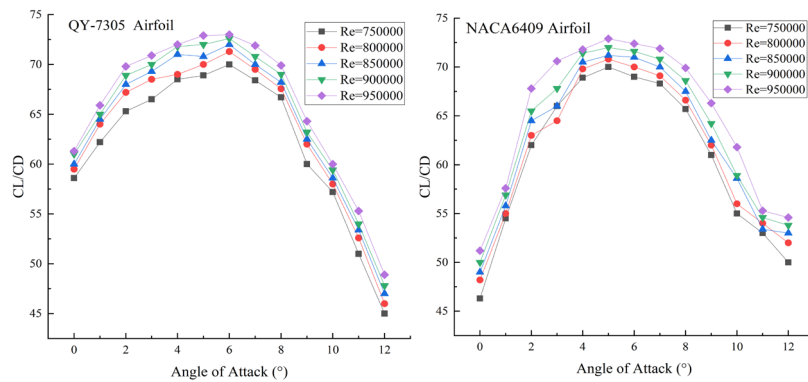


Fig. 9 Lift-to-drag ratio characteristic curves for the airfoil at various Reynolds numbers

### 3. Extraction and aerodynamic performance analysis of the bionic airfoil type of sparrowhawk

#### 3.1 Determination of the overall parameters of the wind turbine

The design parameters of the wind turbine in this paper are shown in Table 1

Table 1

Design parameters of wind turbine blades

Rated power (KW)	Wind turbine drive efficiency $\eta = \eta_1 \times \eta_2$	Wind Energy Utilization Factor Cp	Air density (kg/m <sup>3</sup> )	Design wind speed (m/s)	Number of blades B	Blade tip speed ratio $\lambda_0$	Airfoil Type
44	0.85	0.40	1.225	12	3	6	QY-7305

The diameter of the wind turbine can be determined using the following power equation

$$P = \frac{1}{2} \pi \rho \eta C_p \left( \frac{D^2}{4} \right) V^3 \quad (1)$$

obtained by transforming equation (1)

$$D = \sqrt{\frac{8P}{\pi \rho \eta C_p V^3}} = \sqrt{\frac{8 \times 44000}{\pi \times 1.225 \times 0.85 \times 0.4 \times 12^3}} = 12.5(m)$$

#### 3.2 Establish the mathematical model of blade optimization design method

The Wilson design method, which is based on the blade element theory, divides the blade into equal sections and uses the maximum power coefficient of each section as the objective function for optimization and solution. Increasing the number of segmented elements in the Wilson design method leads to more element cross sections being aligned with the objective function, resulting in a wind turbine blade design that closely approaches an optimal shape and exhibits improved aerodynamic performance. Excessive elements complicate the calculation and modeling process, while insufficient elements compromise accuracy and lead to errors in fitting chord length and twist angle, thereby affecting the optimization of wind turbine blade shape design. This paper proposes a method for non-uniformly acquiring wind turbine blade elements, enabling the adjustment of element numbers within an optimal range to achieve high calculation accuracy. This approach facilitates the creation of 3D models and enhances wind turbine energy utilization. Additionally, relevant correction functions are employed to rectify the calculated

element twist angle and element chord length parameters, thereby providing greater convenience for wind turbine blade design based on the easy 3D model generation.

The basic mathematical model for pneumatic shape calculation is as follows:

Optimal design of wind turbine blades means that the wind turbine has the maximum wind energy utilization factor, even if:

$$dCp = \frac{8}{\lambda_0^2} (1-a)bF\lambda^3 d\lambda \quad (2)$$

Achieving the maximum value under the condition of

$$a(1-aF) = b(1+b)\lambda^2 \quad (3)$$

Where:

$$F = \frac{2}{\pi} \arccos(e^{(-f)}) \quad (4)$$

$$f = \frac{B}{2} \frac{R-r}{R \sin \varphi} \quad (5)$$

After obtaining the induced factors  $a$  and  $b$ , the chord length  $C$  and the installation angle can be obtained by the followairfoil equation  $\theta$ :

$$\tan \varphi = \frac{(1-a)}{(1-b)} \frac{1}{\lambda} \quad (6)$$

$$\theta = \varphi - \alpha \quad (7)$$

$$\frac{BCC_L}{r} = \frac{8\pi a F \sin^2 \varphi}{\cos \varphi} \frac{(1-aF)}{(1-a)^2} \quad (8)$$

$$Re = \frac{V(1-a)C}{\mu \sin \mu} \quad (9)$$

In the above formulas,  $Cp$  is the wind energy utilization coefficient,  $a$  is the axial induction factor,  $b$  is the tangential induction factor,  $F$  is the tip loss factor,  $B$  is the number of blades,  $r$  is the distance from the blade element cross-section to the rotor center,  $\varphi$  is the inflow angle,  $\alpha$  is the angle of attack,  $\theta$  is the twist angle,  $V$  is the incoming wind speed,  $C$  is the chord length,  $C_L$  is the lift

coefficient,  $\mu$  is the dynamic viscosity, and the dynamic viscosity is set to  $1.385 \times 10^{-5} \text{ m}^2/\text{s}$ .

Design steps for the non-uniform adoption of the foliated optimization method:

Firstly, according to the blade element-momentum theory, the wind turbine blade is divided into three parts along the spreading direction, which are blade root, blade middle and blade tip. The spacing between the blade elements at the root is 1.2m, divided into two equal parts; the spacing between the blade elements at the middle of the blade is 0.3m, divided into nine equal parts; the spacing between the blade elements at the tip is 0.9 divided into one equal part; each blade element is a separate airfoil that needs to be calculated. The distribution of blade elements is shown in Figure 10.

For each blade element, the optimization problem is solved using Eq. (2) as the objective function and (3), (4), and (5) as the constraints to determine the induced factors “a” and “b” of the blade element cross section, as well as the slight blade loss factor “F”.

A fitting function is employed to fit the best lift coefficients for different Reynolds numbers to a curve. Using the initial Reynolds number, the initial lift coefficient and chord length are calculated based on Equation (8).

In Figure 9, the optimal angle of attack corresponding to different Reynolds numbers for the QY-7305 airfoil is fitted to a curve using a fitting function. Then, according to equation (9), the Reynolds number is calculated by fitting the obtained curve to determine the optimal angle of attack. The twist angle is obtained using equation (7).

The obtained chord lengths and twist angles are ideal, so it is necessary to make linear corrections to the obtained chord lengths and twist angles in order to make the blades meet the requirements of machining, structure, etc.

Obtain the 3D coordinates of the airfoil sections of each blade element and import the 3D coordinates into Solid works for modeling.

#### 4. Programming and computation

The program is developed using the Wilson optimization design method, and the optimization flowchart is presented in Fig. 11.

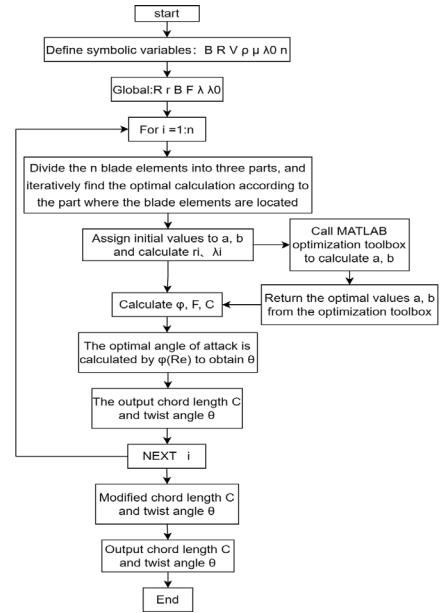
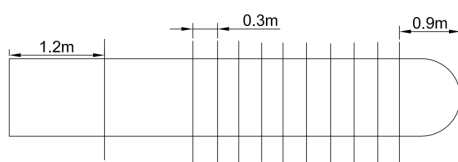


Fig. 10 The blade element distribution chart

Fig. 11 Program flow chart

In the programming, it is important to divide it into three parts: blade root, blade middle, and blade tip. Within the entire loop, if statements are inserted. After calculating the blade root, the various parameters are iterated to calculate the blade middle to prevent inaccurate results due to re-iteration. Similarly, after calculating the blade middle, the parameters are iterated to calculate the blade tip. This process continues until the calculation for the entire blade element is completed.

The iterative calculations lead to the optimization of the chord length and twist angle for each blade element, maximizing the utilization of wind energy. However, in this ideal state, the chord length and twist angle exhibit a nonlinear relationship along the length of the blade, posing challenges in production and processing. To meet the design requirements, fitting operations are necessary to adjust the optimized chord length and twist angle. The Matlab curve fitting function, Polyfit, is utilized for this purpose. It is important to choose an appropriate number of iterations for the fitting process. Too few iterations may result in significant deviation from the optimized parameters and reduced wind energy utilization, while too many iterations may not achieve the desired correction effect, making installation and manufacturing more complex. After careful consideration and practical analysis, a polynomial fitting with a degree of three is applied to correct the chord length and twist angle. The adjustment focuses on the blade elements within the range of 0.4R-0.9R, as wind energy utilization is lower at the

blade root and tip. Additionally, in this range, the blade elements are positioned in the middle portion of the blade and closely spaced, leading to improved fitting results. Matlab software is employed to plot the chord length and twist angle curves before and after the fitting correction, as demonstrated in Fig. 12. Through the analysis of these curves, it can be observed that the fitting results ensure smooth transition in the chord length at the blade tip and provide necessary corrections for excessively large twist angles at the blade root.

Fitting polynomial for the chord length:

$$C(r) = -0.003518r^3 + 0.05453r^2 - 0.325r + 0.9038 \quad (10)$$

Fitting polynomial for the twist angle:

$$\theta(r) = -0.1673r^3 + 2.498r^2 - 14.25r + 29.89 \quad (11)$$

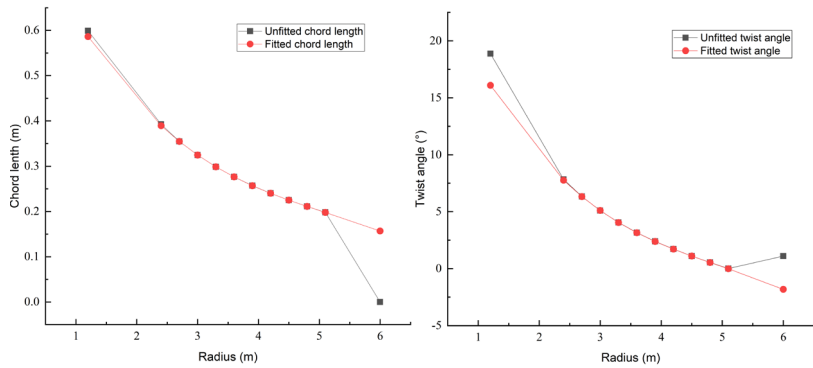


Fig. 12 Chord length and Twist angle fitting curve graph

The optimized values of each prime surface parameter for the blades are presented in Table 2.

Table 2

Parameters of each blade element cross-section of the blade

Radius/m	a	b	Twist angle/°	Fitting twist angle/°	Chord length/m	Fitting chord length/m	F	Re
1.2	0.3351	0.1422	18.88	16.10	0.5990	0.5862	0.9593	790613
2.4	0.3393	0.0387	7.84	7.77	0.3924	0.3893	0.9810	876708
2.7	0.3398	0.0308	6.34	6.33	0.3547	0.3546	0.9822	878994
3	0.3405	0.0251	5.10	5.10	0.3246	0.3246	0.9822	884600
3.3	0.3414	0.0209	4.06	4.06	0.2988	0.2987	0.9811	888609
3.6	0.3427	0.0177	3.17	3.16	0.2765	0.2764	0.9787	891745

3.9	0.3446	0.0152	2.40	2.39	0.2572	0.2570	0.9744	894175
4.2	0.3473	0.0133	1.72	1.71	0.2402	0.2401	0.9673	895912
4.5	0.3513	0.0118	1.11	1.10	0.2250	0.2250	0.9554	896697
4.8	0.3574	0.0107	0.55	0.54	0.2113	0.2111	0.9351	895710
5.1	0.3669	0.0099	0.01	0.00	0.1981	0.1980	0.8989	890634
6	0.1419	0.0039	1.11	-1.82	0.0000	0.1570	0.0000	0

By using the method of coordinate transformation, we first export the two-dimensional coordinates of each blade element section in Profili software, and then use the formula for spatial coordinate transformation to calculate the three-dimensional spatial coordinates of each blade element section. Finally, we import the three-dimensional coordinates of each blade element section into the modeling software to complete the modeling process. The resulting 3D model of the wind turbine is presented in Fig. 13.



Fig. 13 3D model of the wind turbine

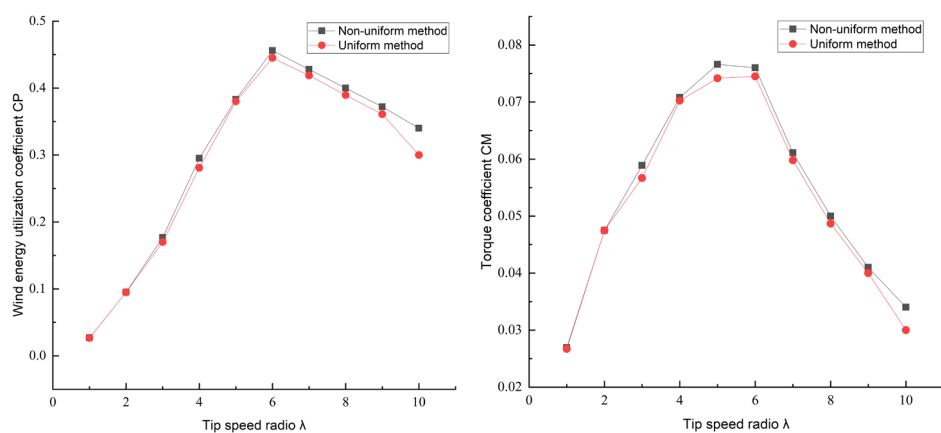
## 5. Analysis of wind turbine blade aerodynamic performance calculation results

Aerodynamic performance calculation plays a crucial role in blade design and verification processes. Verifying its aerodynamic performance becomes an essential step to evaluate the design outcomes. Conversely, the results obtained from aerodynamic performance calculations offer valuable feedback for refining the aerodynamic shape of the blade.

In this study, the aerodynamic performance parameters are computed using the fitting formulas for chord length and twist angle obtained through the non-uniformly sampled blade element method. Additionally, a comparison is performed using the uniformly sampled blade element method for analysis. Both methods utilize twelve cross-sectional blade elements to calculate each parameter, with chord length and twist angle corrections made at 0.4R-0.9R. The resulting aerodynamic performance parameters, such as wind energy utilization coefficient

$C_p$ , torque coefficient  $C_m$ , and thrust coefficient  $C_t$ , are illustrated through curves generated by Matlab, as shown in Fig. 14.

The non-uniform and uniform blade element methods were employed to calculate the coefficient of power ( $C_p$ ), which reached maximum values of 0.4614 and 0.4516, respectively, at a tip speed ratio of 6. The  $C_p$  values obtained using the non-uniform blade element method were consistently higher than those obtained with the uniform blade element method within the tip speed ratio range of 5 to 10. The tip speed ratios align with the design point, reaching their maximum value at 6. Moreover, this study conducted experiments with 10, 15, 20, and 30 blade elements using both methods for comparative analysis. The results indicate that using fewer blade elements leads to improved aerodynamic performance, based on the fitted chord length and twist angle formulas. However, increasing the number of blade elements does not significantly affect the aerodynamic performance parameters. This is primarily due to the fact that employing more blade elements allows both methods to achieve greater accuracy in fitting and correcting the chord length and twist angle within the range of 0.4R to 0.9R. Conversely, when using fewer blade elements, the non-uniform blade element method benefits from smaller intervals in blade element spacing, resulting in higher fitting accuracy for the chord length and twist angle, thus enabling more precise calculations of aerodynamic performance. Therefore, utilizing the non-uniform blade element method not only enhances the aerodynamic performance of the wind turbine blade geometry, but it also mitigates the complexities arising from an excessive number of blade elements in calculations and modeling.



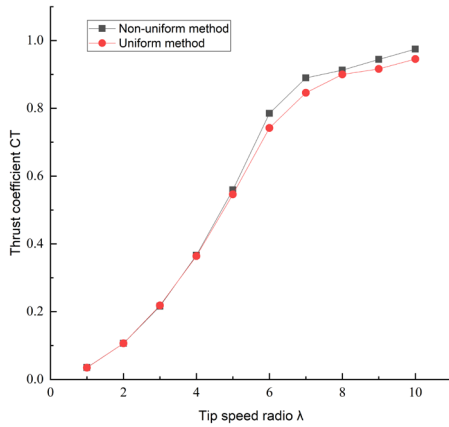


Fig. 14 Cp, Cm, Ct with tip speed ratio

## 6. Conclusion

This study focuses on the sparrowhawk airfoil as the subject of investigation, where a sparrowhawk-inspired airfoil is designed. The lift-to-drag characteristics of the QY-7305 airfoil were compared with those of the NACA6409 airfoil through Computational Fluid Dynamics (CFD) analysis. The blade's parameters are solved using the improved Wilson optimization design method in combination with Matlab software, ensuring the blade's chord length and twist angle fall within 0.4-0.9R(R represents the radius of the wind turbine). The Profili software is employed for exporting the two-dimensional coordinates of each blade element airfoil, while the spatial three-dimensional coordinates (x, y, z) of each blade element cross-section are calculated. A solid blade model is then created with Solidworks software. Subsequently, Matlab software utilizes the fitted chord length and twist angle formula obtained from non-uniformly sampled blade elements to compute the aerodynamic performance parameters. The calculated results are analyzed to derive an optimized design scheme for the wind turbine blades, ensuring the blade meets the targeted design requirements.

## Acknowledgments

**Funding Statement:** This study was supported by the National Natural Science Foundation projects (grant number 51966018), the Chongqing Natural Science Foundation of China (grant number cstc2020jcyj-msxmX0314), the Key Research & Development Program of Xinjiang (grant number 2022B01003), Ningxia Key Research and Development Program of Foreign Science and Techno

logy Cooperation Projects (202204), and the Key Scientific Research Project in Higher Education Institutions from the Ningxia Education Department (2022115).

## R E F E R E N C E S

- [1]. *Badreddinne K, Ali H, David A.* “Optimum project for horizontal axis wind turbines ‘OPHWT’”. *Renewable Energy*, vol. 30, no. 5, 2005, pp. 2019-2043.
- [2]. *Jureczko M, Pawlak M, Mezyk A.* “Optimisation of wind turbine blades”. *Journal of Materials Processing Technology*, vol. 167, no.2-3, 2005, pp. 463-471.
- [3]. *Rajakumar S, Ravindran D.* “Iterative approach for optimizing coefficient of power, coefficient of lift and drag of wind turbine rotor”. *Renewable Energy*, vol. 38, no.1, 2012, pp. 83-93.
- [4]. *Lanzafame R, Messina M.* “Design and performance of a double-pitch wind turbine with non-twisted blades”. *Renewable Energy*, vol.34, no. 5, 2009, pp. 1413-1420.
- [5]. *Y. Zhiqiang, Y. Minghui, C. Xiaoyang, C. Zaiyu and Z. Yun*, “Multi-AOA optimization of variable-speed wind turbine airfoils,” 2016 IEEE Region 10 Conference (TENCON), Singapore, 2016, pp. 1674-1677.
- [6]. *Yuan K S, Li N R.* “Analysis Influence of Trailing Edge Modification on Aerodynamic Performance of Airfoils for Wind Turbine”. *Applied Mechanics and Materials*, vol. 220, 2025, pp. 900-904.
- [7]. *Huang S, Hu Y, Wang Y.* “Research on aerodynamic performance of a novel dolphin head-shaped bionic airfoil”. *Energy*, vol. 214, 2020, pp. 118179.
- [8]. *Hua X, Zhang C, Wei J, et al.* “Wind turbine bionic blade design and performance analysis”. *Journal of Visual Communication and Image Representation*, vol. 60, no. C, 2019, pp. 258-265.
- [9]. *Tian W, Yang Z, Zhang Q, et al.* “Bionic design of wind turbine blade based on long-eared owl’s airfoil”. *Applied Bionics and Biomechanics*, vol. 2017, no. 1, 2017, pp1-10.
- [10]. *L. Wenzhi, W. Jianxin, Z. Fuhai and L. Changzeng*, “3D Modeling Methods of Aerodynamic Shape for Large-Scale Wind Turbine Blades”, 2009 International Conference on Information Technology and Computer Science, Kiev, Ukraine, 2009, pp. 7-10.
- [11]. *Yan H, Su X, Zhang H, et al.* “Design approach and hydrodynamic characteristics of a novel bionic airfoil”. *Ocean Engineering*, vol. 216, 2020, pp. 108076.
- [12]. *Hassanzadeh A, Hassanabad A H, Dadvand A.* “Aerodynamic shape optimization and analysis of small wind turbine blades employing the Viterna approach for post-stall region”. *Alexandria Engineering Journal*, vol. 55, no.3, 2016, pp. 2035-2043.
- [13]. *Lee, S.-L., Shin, S.* “Wind Turbine Blade Optimal Design Considering Multi-Parameters and Response Surface Method”. *Energies*. Vol. 13, no. 7, 2020, pp. 1639-1662.

- [14]. *Li Q, Jin Z, et al.* “Review of aerodynamic shape optimization design of wind turbine blades”. Mechanical design. vol. 33, no. 07, 2016, pp. 1-7.
- [15]. *Rodriguez Christian V, Celis Cesar.* “Design optimization methodology of small horizontal axis wind turbine blades using a hybrid CFD/BEM/GA approach”. Journal of the Brazilian Society of Mechanical Sciences and Engineering, vol. 44, no. 6, 2022, pp. 254.
- [16]. *Zhu, Jie, Cai X.; Gu, R.* “Aerodynamic and Structural Integrated Optimization Design of Horizontal-Axis Wind Turbine Blades”. Energies. Vol. 9, no. 02, 2016, pp. 66-84.
- [17]. *Zhang B, Song B, Mao Z, Tian W, Li B, Li B.* “A Novel Parametric Modeling Method and Optimal Design for Savonius Wind Turbines”. Energies. Vol. 10, no. 3, 2017, pp. 301-321.
- [18]. *Maki K, Sbragio R, Vlahopoulos N.* “System design of a wind turbine using a multi-leval optimization approach”. Renewable Energy, vol.43, 2012, pp. 101-110.
- [19]. *Tang X, Huang X, Peng R, et al.* “A Direct Approach of Design Optimization for Small Horizontal Axis Wind Turbine Blades”. Procedia CIRP, vol. 36, 2015, pp.12-16.